

# Identifying Strong-Field Effects in Indirect Photofragmentation Reactions

Chuan-Cun Shu,<sup>\*,†</sup> Kai-Jun Yuan,<sup>‡,¶</sup> Daoyi Dong,<sup>¶,§</sup> Ian R. Petersen,<sup>†</sup> and  
Andre D. Bandrauk<sup>\*,‡</sup>

<sup>†</sup>*School of Engineering and Information Technology, University of New South Wales, Canberra,  
ACT 2600, Australia*

<sup>‡</sup>*Laboratoire de Chimie Théorique, Faculté des Sciences, Université de Sherbrooke Sherbrooke  
(Québec) J1K 2R1, Canada*

<sup>¶</sup>*School of Engineering and Information Technology, University of New South Wales, Canberra,  
Australian Capital Territory 2600, Australia*

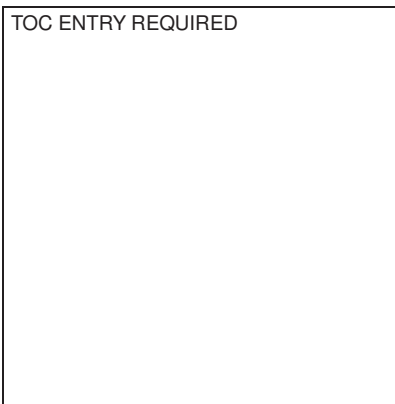
<sup>§</sup>*Department of Chemistry, Princeton University, Princeton, New Jersey 08544, USA*

E-mail: c.shu@unsw.edu.au; andre.bandrauk@usherbrooke.ca

## Abstract

Exploring molecular breakup processes induced by light-matter interactions has both fundamental and practical implications. However, it remains a challenge to elucidate the underlying reaction mechanism in the strong field regime, where the potentials of the reactant are modified dramatically. Here, we perform a theoretical analysis combined with a time-dependent wavepacket calculation to show how a strong ultrafast laser field affects the photofragment products. As an example, we examine the photochemical reaction of breaking up the molecule NaI into the neutral atoms Na and I, which due to inherent nonadiabatic couplings is indirectly formed in a stepwise fashion via the reaction intermediate NaI\*. By analyzing the angular dependencies of fragment distributions, we are able to identify the reaction intermediate NaI\* from the weak to the strong field-induced nonadiabatic regimes. Furthermore, the energy levels of NaI\* can be extracted from the quantum interference patterns of the transient photofragment momentum distribution.

## Graphical TOC Entry



Since the scientist Ahmed Zewail (1946-2016) was awarded the 1999 Nobel Prize in Chemistry for his work on femtochemistry, controlling chemical reactions by employing light as a “photonic reagent” has become a long-standing target going beyond traditional approaches using heat or catalysts.<sup>1-6</sup> One type of photochemical reaction is the dissociation of a molecule into fragments,<sup>7</sup> which for example plays an important role in energy transfer processes during the light reaction of photosynthesis.<sup>8</sup> There has been considerable theoretical and experimental interest in the study of such processes in both diatomic and polyatomic molecular systems.<sup>9-17</sup> Photodissociation dynamics can be broadly classified as direct and indirect processes,<sup>7</sup> which can be identified by using a potential energy surface concept. For a direct fragmentation reaction, an excited wavepacket evolves following a purely repulsive potential, from which the molecule can fly apart immediately on an ultrafast time-scale smaller than a typical internal vibrational period. For an indirect fragmentation reaction, the potential of the excited state involved is not purely repulsive, where the excited wavepacket may survive for a sufficiently long time from several to thousands of internal vibrational periods.

It is very difficult to gain an insight into photochemical reactions in the presence of strong fields, where the molecular Hamiltonian associated with electronic, vibrational and rotational energy levels is significantly modified by the applied fields. By considering field-dressed Born-Oppenheimer potentials, the concept of light-induced potential (LIP)<sup>18-21</sup> is often used to interpret various strong-field-induced phenomena including bond softening,<sup>22</sup> bond hardening<sup>23</sup> and above-threshold dissociation.<sup>24,25</sup> An intriguing approach regarding LIPs investigates the creation of light-induced conical intersection (LICI) in diatomic molecules,<sup>26-28</sup> which cannot form a natural conical intersection (CI) under field-free conditions. Considerable theoretical approaches have examined the impact of LICI on the direct fragmentation reaction,<sup>29-33</sup> and has demonstrated the existence of LICI in diatomic molecules.<sup>34</sup> However, these strong-field-induced phenomena are largely unexplored in the case of indirect fragmentation reactions. In this Letter, we show how a strong ultrafast laser pulse affects indirect photofragment distributions of diatomic molecules in the photochemical reaction  $AB \xrightarrow{\text{laser}} (AB)^* \rightarrow A+B$ , which in turn provides a new approach to identify quantum

energy level structures of the reaction intermediate  $AB^*$  from photochemical reaction products.

As a prototype system, we focus on the indirect photodissociation reaction of the molecule NaI, which consists of the ground ionic state of  $Na^+I^-$  and the lowest covalent excited state NaI. The corresponding diabatic potential curves, ground  $V_g(R)$  and excited  $V_e(R)$ , interact with each other nonadiabatically around their crossing at an internuclear distance of  $R_c \approx 6.93 \text{ \AA}$ ,<sup>35</sup> where an avoided covalent-ionic curve crossing via a nondiabatic coupling  $V_c(R)$  is formed. We consider the molecule to be excited by a linearly polarized ultrafast laser pulse, whose electric field vector is described by  $\mathbf{E}(t) = \hat{\mathbf{e}}_z \mathcal{E}_0 f(t) \cos \omega_0 t$  with the carrier frequency  $\omega_0$ , peak amplitude  $\mathcal{E}_0$ , pulse envelope  $f(t)$  and polarization direction  $\hat{\mathbf{e}}_z$ . The molecular Hamiltonian  $\hat{H}(t)$  using the electric-dipole approximation can be given by

$$\hat{H}(t) = \begin{pmatrix} -\frac{1}{2\mu} \frac{\partial^2}{\partial R^2} + \frac{\hat{J}^2}{2\mu R^2} & 0 \\ 0 & -\frac{1}{2\mu} \frac{\partial^2}{\partial R^2} + \frac{\hat{J}^2}{2\mu R^2} \end{pmatrix} + \begin{pmatrix} V_g(R) & -d(R) \cos \theta \mathcal{E}_0 f(t) \cos \omega_0 t + V_c(R) \\ -d(R) \cos \theta \mathcal{E}_0 f(t) \cos \omega_0 t + V_c(R) & V_e(R) \end{pmatrix}, \quad (1)$$

where  $\hat{J}^2$  is the angular momentum operator of the nuclear rotation,  $\theta$  the angle between the molecular axis and the laser field polarization direction  $\hat{\mathbf{e}}_z$ , and  $d(R)$  the transition dipole moment between the two diabatic electronic states. After diagonalizing the diabatic potential energy matrix in Eq. (1), two time-dependent LIPs,  $V_g^{LIP}(R, \theta, t)$  and  $V_e^{LIP}(R, \theta, t)$  can be written in the adiabatic representation as

$$V_g^{LIP}(R, \theta, t) = \frac{1}{2} \left[ V_e(R) - \hbar\omega_0 + V_g(R) - \sqrt{\Delta^2 + 4C^2(t)} \right], \quad (2a)$$

and

$$V_e^{LIP}(R, \theta, t) = \frac{1}{2} \left[ V_e(R) - \hbar\omega_0 + V_g(R) + \sqrt{\Delta^2 + 4C^2(t)} \right], \quad (2b)$$

where the detuning  $\Delta$  is given by  $\Delta = V_e(R) - \hbar\omega_0 - V_g(R)$ , and the total nondiabatic coupling  $C(t)$  is defined as  $C(t) = -\frac{1}{2}d(R)\mathcal{E}_0 f(t) \cos \theta + V_c(R)$ . A detailed description of diabatic and adiabatic representations can be found in Ref.<sup>36</sup> The two LIPs are degenerate, whenever  $\Delta = 0$  and  $C(t) = 0$

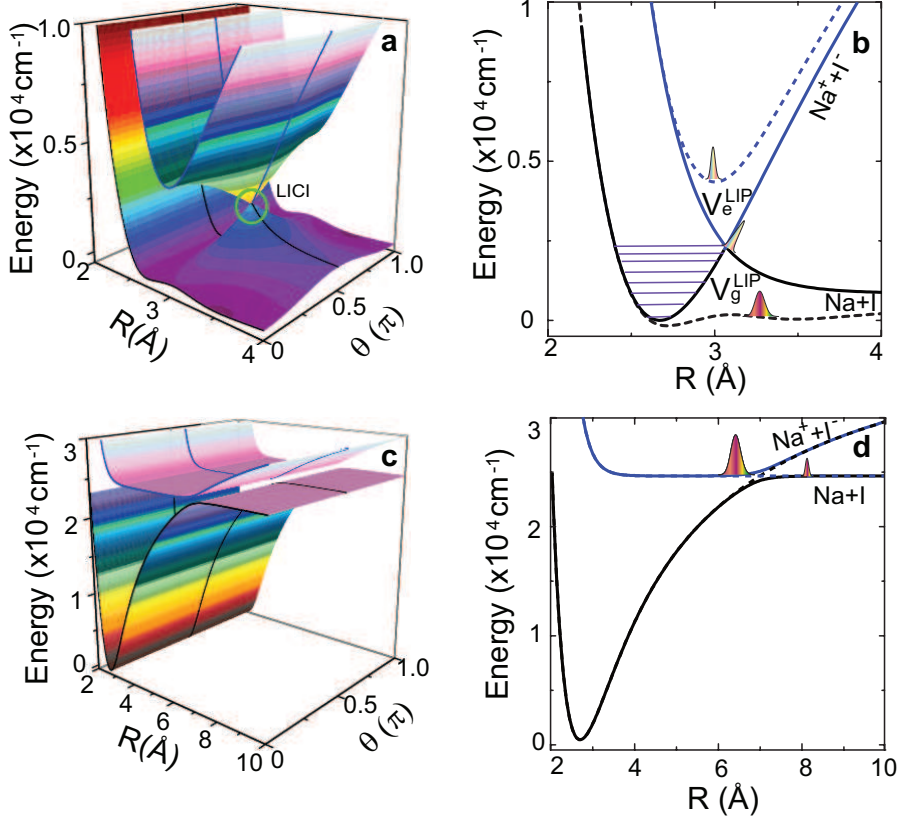


Figure 1: Schematic illustration of the photodissociation reaction of NaI. **a** The light-induced potentials (LIPs) and **c** the field-free potential energy surfaces of the molecule NaI as a function of the internuclear distance  $R$  and the angle  $\theta$  between the molecular axis and the laser polarization direction. **b** A cut through the LIPs at  $\theta = 0$  (dashed lines) and  $\pi/2$  (solid lines), where  $V_g^{LIP}$  and  $V_e^{LIP}$  are coloured in dark and blue, respectively. **d** The diabatic potentials for the ground ionic state (black dashed line) and the lowest covalent excited state (the blue dashed line), and the adiabatic potentials for the ground electronic state (black solid line) and the excited electronic state (blue solid line). The green circle in **a** highlights the light-induced conical intersection (LICI) region. The wave packet trapped in the upper adiabatic potential corresponds to the reaction intermediate  $\text{NaI}^*$ .

are fulfilled simultaneously. As the nondiabatic coupling  $V_c(R)$  for the molecule NaI is negligible in the Franck-Condon region, the condition  $C(t) = 0$  always holds at  $\theta = \pi/2$  (i.e.,  $\cos \theta = 0$ ). As a result, the LICI can be formed in the covalent molecule NaI, and its position is determined by the carrier frequency  $\omega_0$ .

Figure 1a shows  $V_g^{LIP}(R, \theta)$  and  $V_e^{LIP}(R, \theta)$  at  $\hbar\omega_0 = 24390 \text{ cm}^{-1}$  (410 nm). The gap between the two LIPs at a given internuclear distance  $R$  is maximal at the angles  $\theta = 0$  and  $\pi$ , whereas it vanishes at the angle  $\theta = \pi/2$  and the internuclear distance  $R = R_{CI} \approx 3.1 \text{ \AA}$ . To explore how

the two different LIPs as well as the LICIs play roles, as sketched in Figure 1 b, we prepare the molecular system initially in a high vibrational level of the ground electronic state, so that the excited wavepackets evolve simultaneously on both  $V_g^{LIP}$  and  $V_e^{LIP}$ . The lower LIP  $V_g^{LIP}$  correlates  $V_g$  to  $V_e$  at large  $R$  ( $> R_{CI}$ ), whereas the upper LIP  $V_e^{LIP}$  connects  $V_g$  to  $V_e$  at small  $R$  ( $< R_{CI}$ ). Since there is no internal barrier, the field-induced bound states are created in  $V_e^{LIP}$ , resulting in a vibrational trapping, i.e., chemical bond hardening.<sup>23</sup> In the vicinity of the LICIs, the gap between the two LIPs is small, giving rise to a nonadiabatic transition to the resonance states of  $V_e$ , which is similar to the weak-field one-photon resonance excitation.

We first analytically examine how the excited wavepacket evolves after these LIPs as well as LICIs disappear. Under the field-free condition the inherent nondiabatic coupling  $V_c(R)$  results in two adiabatic curves  $V_g^{ad}(R)$  and  $V_e^{ad}(R)$  with a trapping well in the upper excited state, as shown in Figures 1c and d. Different from the direct fragmentation reaction, the excited nuclear wavepacket, i.e., the reaction intermediate  $\text{NaI}^*$ , performs oscillating motions in the excited adiabatic electronic state  $V_e^{ad}$ , resulting in indirect dissociation along the  $\text{Na}+\text{I}$  channel in a stepwise fashion.<sup>2,35</sup> The coherent superposition of quasibound states  $\text{NaI}^*$  can be expanded as

$$|\Psi_e^{ad}(t)\rangle = \sum_{\nu, J} c_{\nu J} |E_\nu\rangle e^{-iE_\nu t/\hbar} |E_{JM}\rangle e^{-iE_{JM} t/\hbar}, \quad (3)$$

where  $|E_\nu\rangle$  is the vibrational eigenstate with the vibrational quantum number  $\nu$ ,  $|E_{JM}\rangle$  is the rotational eigenstate with the rotational quantum numbers  $J$  and  $M$ ,  $c_{\nu J}$  denotes the corresponding expansion coefficient of the rovibrational state  $|E_\nu E_{JM}\rangle$ . For linearly polarized light case, the quantum number  $M$  is conserved, and therefore the rotational state  $|E_{JM}\rangle$  of the molecule can be described by the associated-Legendre polynomial  $P_J^M(\cos\theta)$ . When such a wavepacket approaches the nonadiabatic coupling region  $R \approx R_c$ , the quasibound states will decay to the continuum via the nondiabatic coupling  $V_c$ . The ‘‘leaked out’’ wave packet in the continuum states can be described by<sup>37,39</sup>  $|\Psi_e(t)\rangle = -\frac{i}{\hbar} \int_0^t dt' \hat{U}_0(t, t') V_c |\Psi_e^{ad}(t')\rangle$ , where  $\hat{U}_0(t, t')$  is the field-free evolution operator of the system.

The probability of observing fragments in an eigenstate  $|E, p\rangle$  along the direction  $\theta$  at the time  $t$  can be given by

$$P(E, \theta, t) \equiv |\langle E, p | \Psi_e(\theta, t) \rangle|^2 \propto \left| \sum_{vJ} c_{vJ} V_{vJME} \frac{e^{-(E_v + E_{JM})t/\hbar} - 1}{(E_v + E_{JM} - E)/\hbar} P_J^M(\cos \theta) \right|^2 \quad (4)$$

where  $V_{vJME} = \langle E, p | V_c | E_v E_{JM} \rangle$  denotes the coupling matrix elements between the resonant state  $|E_v E_{JM}\rangle$  and the continuum state  $|E, p\rangle$ , with the total energy of the fragments  $E = p^2/2\mu + D_0$  and the dissociation energy  $D_0$  of Na+I. A further analysis of Eq. (4) predicts that the energy distribution consists of multiple peaks centered at  $E_v + E_{JM}$  weighted by the expansion coefficient  $c_{vJ}$  and the coupling matrix element  $V_{vJME}$  at the corresponding energy, and such a time-dependent distribution exhibits low energy resolution at short times.<sup>37,39</sup> The components of the excited resonance states  $|E_v E_{JM}\rangle$  of NaI\* in the weak light-molecule interaction regime can be approximated via first-order perturbation theory by

$$c_{vJ} = \langle E_{JM} E_v | d \cos \theta | \epsilon_0 \rangle \int_{-\infty}^{\infty} dt \mathcal{E}_0 f(t) \cos \omega_0 t e^{i\omega_{E_v J_0} t}, \quad (5)$$

where  $\omega_{E_v J_0} = (E_v + E_{JM} - \epsilon_0)/\hbar$ , and  $|\epsilon_0\rangle$  is the initial rovibrational state of the system with the eigenenergy  $\epsilon_0$ , and therefore are determined by a product of the Franck-Condon factor and the laser pulse frequency distribution at the transition frequency. In the presence of strong light-molecule interactions, the excited quasibound states  $|E_v E_{JM}\rangle$  will be modified going beyond first-order perturbation theory, but as seen from Eq. (4) the expansion coefficients  $c_{vJ}$  can be extracted from indirect photofragment distributions.

In the following we perform a time-dependent quantum wavepacket calculation to examine how such an excited wavepacket, i.e., the reaction intermediate NaI\*, is unfolded in real time. The propagation of the wavepackets  $\Psi_g(R, \theta, t)$  and  $\Psi_e(R, \theta, t)$  with the two diabatic potentials  $V_g(R)$  and  $V_e(R)$  is obtained by solving the time-dependent Schrödinger equation (TDSE) with the Hamiltonian in Eq. (1). The linearly polarized laser field  $\mathbf{E}(t)$  is taken to be an experimentally accessible

Gaussian transform limited pulse centered at  $t = 0$  with the full-width at half-maximum (FWHM) of 30 fs. The center wavelength of the laser pulse is fixed at 410 nm, and throughout the calculations the initial nuclear wave function was assumed to be in a single eigenstate of the ground electronic state with the vibrational quantum number of  $\nu = 7$  and the rotational quantum number of  $J = 0$ . The wave functions, potentials, and coupling element are represented on an equally spaced grid of 8192 points with  $1.5 \leq R \leq 93 \text{ \AA}$ . An absorbing potential is added for  $R \geq 92 \text{ \AA}$  to avoid unphysical reflections into the inner region. The data for the potential energy surfaces  $V_g(R)$  and  $V_e(R)$ , the transition dipole moments  $d(R)$  and the nonadiabatic coupling  $V_c(R)$  can be found in literature.<sup>35</sup> Since the used laser frequency is far from resonances with vibrational and rotational transitions within the same electronic state, the transitions induced by the permanent dipole moments are negligible. The further details for numerically solving TDSE can be found in Refs.<sup>37,38</sup>

The time-dependent momentum distribution of the photofragments  $\text{NaI}^* \rightarrow \text{Na} + \text{I}$  is computed by Fourier transforming the wavefunction  $\Psi(R, \theta, t)$  from position space to momentum space as

$$\Phi(p, \theta, t) = \frac{1}{\sqrt{2\pi\hbar}} \int_{-\infty}^{\infty} \exp\left(-\frac{ipR}{\hbar}\right) g(R) \Psi_e(R, \theta, t) dR, \quad (6)$$

where  $g(R)$  is a filter function that will effectively suppress the part of the wavepacket in the avoided crossing region and becomes a constant of 1 in the asymptotic dissociation region. In our simulations, we take  $g(R) = 1 - \exp[-a(R - R_d)]$  for  $R > R_d$  and  $g(R) = 0$  for  $R < R_d$  with  $a = 0.4 \text{ \AA}^{-1}$  and  $R_d = 10 \text{ \AA}$ . Such time-dependent momentum distributions can be measured practically in experiment based on the technology of transient momentum imaging of photofragments.

Figure 2 shows the angular distributions of the fragment momentum at  $t = 0.8$  ps, corresponding to one outgoing fragment. For comparison, the simulations are accomplished by using a weak laser pulse at the peak intensity of  $I_0 = 1.0 \times 10^{12} \text{ W/cm}^2$  and a strong one at  $I_0 = 3.0 \times 10^{13} \text{ W/cm}^2$ , respectively. In the weak field case, the initial rovibrational state  $|\nu = 7, J = 0\rangle$  via one-photon transitions is coupled to the resonant state  $|E_\nu\rangle$  with  $\Delta J = \pm 1$ , which as predicted in Eq. (4) produces a  $\cos^2 \theta$  (i.e.,  $|P_1^0(\cos \theta)|^2$ ) distribution. As seen from Figure 2a, the fragment momen-

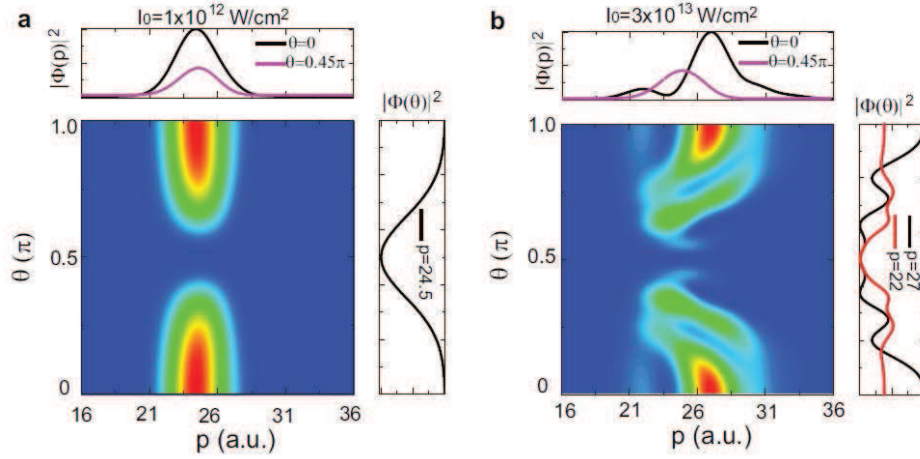


Figure 2: Probability distributions for relative momentum of Na+I. The results, i.e.,  $|\Phi(p, \theta, t)|^2$ , are observed at  $t = 0.8$  ps, corresponding to one outgoing fragment, with **a** the weak-field case at  $I_0 = 1.0 \times 10^{12}$  W/cm<sup>2</sup>, and **b** the strong field case at  $I_0 = 3.0 \times 10^{13}$  W/cm<sup>2</sup>.

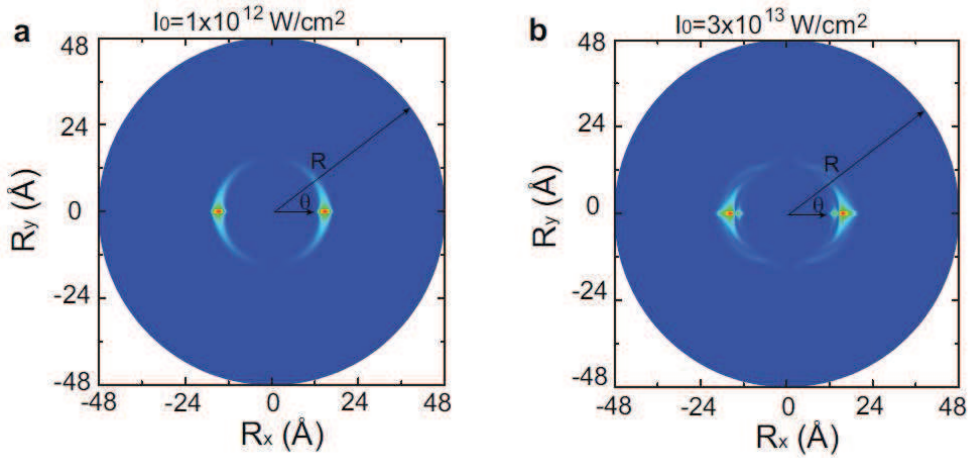


Figure 3: Probability distributions for the wavepackets of photofragments. The results are observed in the asymptotic dissociation region  $|g(R)\Psi_e(R, \theta, t)|^2$  at  $t = 0.8$  ps, with **a** the weak-field case at  $I_0 = 1.0 \times 10^{12}$  W/cm<sup>2</sup>, and **b** the strong field case at  $I_0 = 3.0 \times 10^{13}$  W/cm<sup>2</sup>.

tum exhibits a Gaussian-like distribution with the maximum value around  $p = 24.5$  a. u. (i.e.,  $\sqrt{2\mu(\epsilon_0 + \hbar\omega_0 - D_0)}$ ), in good agreement with the theoretical analysis in Eqs. (4) and (5). The photofragment distributions are obviously changed in the strong field case as compared with those in the weak-field case, see Figure 2b. Two separated peaks around  $p = 22$  and  $27$  a.u. are produced in the strong laser-induced nonadiabatic coupling regions ( $\theta \rightarrow 0$ , and  $\pi$ ), whereas a Gaussian-like envelop with the maximum around  $p = 24.5$  a.u. appears again in the weak coupling region

$(\theta \rightarrow \pi/2)$ .

The photofragment distribution as indicated in Eq. (4) directly reflects the quasibound states of the excited electronic states. In Figure 2b the two shifted and separated peaks thus imply that the quasibound states below and above the resonant states are excited simultaneously. In the LIP representation, the blue-shifted peaks around  $p = 27$  a.u. correspond to the product from the lower LIP  $V_g^{LIP}$  passage, which brings the system from the initial state to the higher quasibound states of  $V_e$ . The red-shifted peaks around  $p = 22$  a.u. comes from the upper LIP  $V_e^{LIP}$ , which moves the system from the initial state to those quasibound states below resonant states. The shifted value of the momentum at a given direction  $\theta$  can be predicated by Eq. (2) with  $\Delta p = \pm \sqrt{\mu d(R) \mathcal{E}_0 \cos \theta}$  at  $R = R_{CI}$ . Figure 3 plots the probability density distribution of the dissociating fragments  $|g(R)\Psi_e(R, \theta, t)|^2$  on a “disk” for both the weak and strong field cases. Comparing to the weak field case with a single-“crescent-like” distribution (Figure 3a), a double-“crescent-like” distribution around  $\theta = 0$  and  $\pi$  (Figure 3b) is induced in the strong field case, indicating that two different manifolds of quasibound states are included. In addition, both the momentum and probability density distributions consistently establishes that the fragmentats from the higher quasibound states dominates. This can be attributed to two main reasons: one is that more initial wavepackets are excited along the lower adiabatic LIP to the higher quasibound states, and the other is that the inherent nonadiabatic coupling  $V_{vJME}$  in Eq. (4) may suppress the lower quasibound states to cross over the avoided crossing region.

We now examine the fragment distributions at  $t = 1.2$  ps in Figures 4 and 5, corresponding to two outgoing fragments. As indicated in Eq. (4), quantum interferences in the momentum distributions are found in both the weak and the strong field cases. The spacing between the momentum lines around the center corresponds to  $\sim 59 \text{ cm}^{-1}$ , in good agreement with the known energy spacing between the quasibound energy levels of  $\text{NaI}^*$ . Since the transient momentum spectrum is calculated after the laser pulse, the observed energy spacing is independent of laser intensity. As shown in Figure 5, two well-separated wave-packets appear in the dissociation asymptotic region. Since the two space-separated wavepackets come from the same “source”, i.e., the reaction inter-

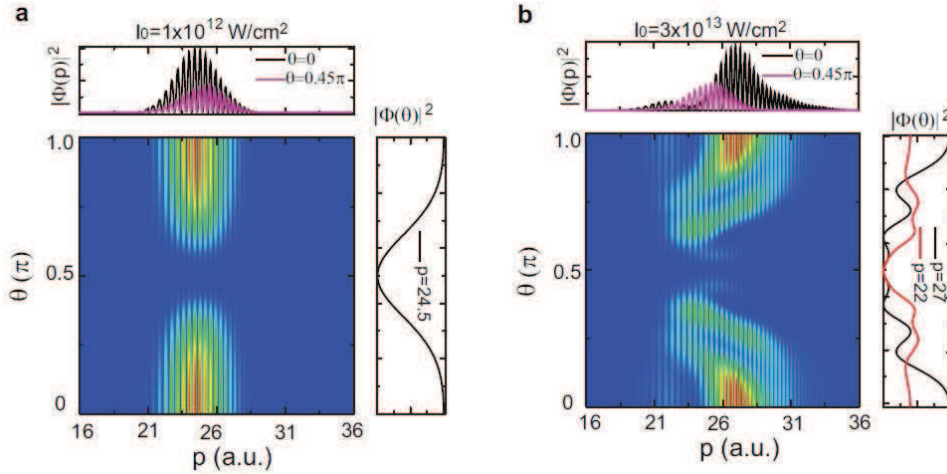


Figure 4: Probability distributions for relative momentum of Na+I. The results, i.e.,  $|\Phi(p, \theta, t)|^2$ , are observed at  $t = 1.2$  ps, corresponding to two outgoing fragments with **a** the weak-field case at  $I_0 = 1.0 \times 10^{12}$  W/cm<sup>2</sup>, and **b** the strong field case at  $I_0 = 3.0 \times 10^{13}$  W/cm<sup>2</sup>.

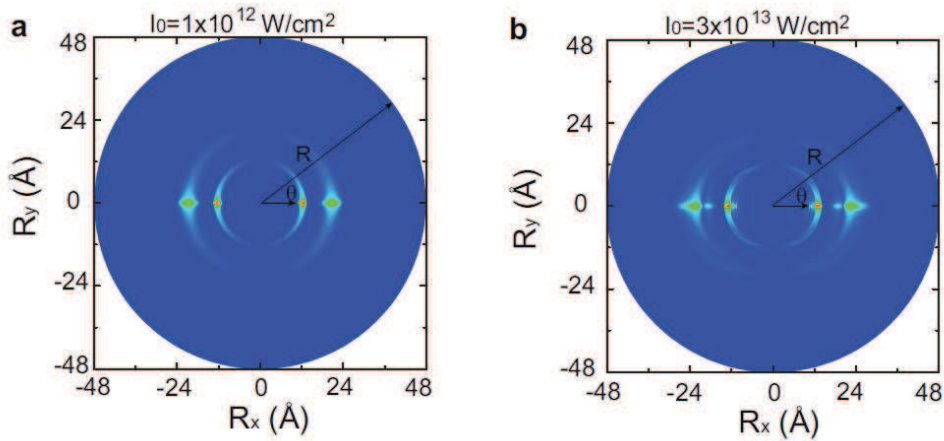


Figure 5: Probability distributions for the wavepackets of photofragments. The results are observed in the asymptotic dissociation region  $|g(R)\Psi_e(R, \theta, t)|^2$  at  $t = 1.2$  ps, with **a** the weak-field case at  $I_0 = 1.0 \times 10^{12}$  W/cm<sup>2</sup>, and **b** the strong field case at  $I_0 = 3.0 \times 10^{13}$  W/cm<sup>2</sup>.

mediate NaI\* associated with the trapped wavepacket, they can create quantum interference in the momentum space. In the region near  $\theta = \pm\pi/2$ , the separated wavepackets only show a single “crescent-like” distribution, and the corresponding momentum distributions are again similar to the weak field case. The interference patterns observed in Figure 4 provide a direct signature to distinguish the indirect dissociation reaction from the direct one, where the excited molecule will not be trapped under the field-free condition. Note that the wavepacket after 1.2 ps (as shown in

Figure 5) is just spread to the region of  $R \leq 36 \text{ \AA}$  far from the boundary, indicating that there is no influence of the absorbing potential on the accuracy of the calculations.

It is interesting to note that in the strong field case the angular distributions of the photofragments at a given momentum become complex, going beyond those in the weak field case. This rotational structure can be explained by Eq. (4), i.e., due to the strong-field-molecule interaction, more than one rotational state associated with higher order  $P_J^M(\cos \theta)$  contribute to the fragment distributions. This mechanism is different from quantum interference effects caused by the existence of the LICl, which has been observed in direct photofragmentation reactions for example in the molecule ions,  $\text{H}_2^+$  and  $\text{D}_2^+$ .<sup>26,34</sup> In the present case for the molecule NaI, the field-molecule interaction time ( $< 100 \text{ fs}$ ), as compared with the rotational period of the excited wavepackets (basic rotational period of NaI is  $138 \text{ ps}$ ), is too short to rotate the molecule in the upper LIP to the vicinity of the LICl. As a result, there is almost no the excited wavepacket that undergoes nonadiabatic transitions from the upper LIP to the higher quasibound states which can interfere with the wavepacket along the lower LIP  $V_g^{LIP}$ .

In summary, we have investigated how strong-laser-field-modified molecular potentials play a role in indirect photofragmentation reactions. A theoretical analysis combined with the time-dependent wavepacket simulations was applied to the photochemical reactions of breaking up the molecule NaI into the neutral atoms Na and I through the reaction intermediate  $\text{NaI}^*$ . We have identified that the photofragment distributions are produced upon laser-induced quasibound states  $\text{NaI}^*$ , and shown that the energies of these quasibound states  $\text{NaI}^*$  can be extracted from the transient photofragment momentum distributions. These results provide a new approach to gain an insight into the reaction intermediate directly from photochemical reaction products, and this method in principle can be extended to study more complex molecular systems. Although the present work highlighted how a single strong laser field affects the reaction intermediate, it is also interesting to explore how commonly used coherent control schemes can be employed to control the reaction intermediate. To this end, we may use a second either resonant or nonresonant pulse to further excite the wavepacket of the reaction intermediate. Furthermore, the scheme presented in this work can

also be transposed to examine indirect dissociation in the case of photo-predissociation involving multiple electronic excited states.

## Author information

### Corresponding Author

\*(C.C.S) Email:c.shu@unsw.edu.au

\*(A.D.B) Email:andre.bandrauk@usherbrooke.ca

### Notes

The authors declare no competing financial interest.

## Acknowledgement

C.C.S. acknowledges the financial support by the Vice-Chancellor's Postdoctoral Research Fellowship of The University of New South Wales, Australia. K.J.Y. acknowledges the support and hospitality provided by UNSW Canberra during his visit. D.D. and I.R.P. acknowledge partial supports by the Australian Research Council under Grant Nos. DP130101658 and FL110100020. The authors also thank RQCHP and Compute Canada for access to massively parallel computer clusters.

## References

- (1) Zewail, A. H. Femtochemistry: Atomic-Scale Dynamics of the Chemical Bond. *J. Phys. Chem. A* **2000**, *104*, 5660-5694.
- (2) Mokhtari, A.; Cong, P.; Herek, J. L.; Zewail, A. H. Direct Femtosecond Mapping of Trajectories in a Chemical Reaction. *Nature* **1990**, *348*, 225-227.

- (3) Rabitz, H.; Motzkus, M.; Kompa, K.; de Vivie-Riedle, R. Whither the Future of Controlling Quantum Phenomena? *Science* **2000**, *288*, 824-828.
- (4) Skubi, K. L.; Yoon, T. P. Organic Chemistry: Shape Control in Reactions with Light. *Nature* **2014**, *515*, 45-46.
- (5) Huo, H.; Shen, X.; Wang, C.; Zhang, L.; Röse, P.; Chen, L.-A.; Harms, K.; Marsch, M.; Hilt, G.; Meggers, E. Asymmetric Photoredox Transition-Metal Catalysis Activated by Visible Light. *Nature* **2014**, *515*, 100-103.
- (6) Meyer, K.; Liu, Z.; Müller, N.; Mewes, J.-M.; Dreuw, A.; Buckup, T.; Motzkus, M.; Pfeifer, T. Signatures and Control of Strong-Field Dynamics in a Complex System. *Proc. Natl. Acad. Sci.* **2015**, *112*, 15613-15618.
- (7) Schinke, R. *Photodissociation Dynamics*; Cambridge University Press: Cambridge, U.K.; 1993.
- (8) Engel, G. S.; Calhoun, T. R.; Read, E. L.; Ahn, T.-K.; Mancaronal, T.-C.; Cheng, Y.-C.; Blankenship, R. E.; Fleming, G. R. Evidence for Wavelike Energy Transfer through Quantum Coherence in Photosynthetic Systems. *Nature* **2007**, *446*, 782-786.
- (9) Sussman, B. J.; Townsend, D.; Yu, Ivanov, M.; Stolow, A. Dynamic Stark Control of Photochemical Processes. *Science* **2006**, *314*, 278-281.
- (10) Corrales, M. E.; González-Vázquez, J.; Balardi, G.; Solá, I. R.; de Nalda, R.; Bañares, L. Control of Ultrafast Molecular Photodissociation by Laser-Field-Induced Potentials. *Nature Chem.* **2014**, *6*, 785-790.
- (11) Bargheer, M.; Gerber, R. B.; Korolkov, M. V.; Kühn, O.; Manz, J.; Schröder M.; Schwentner N. Subpicosecond Spin-Flip Induced by the Photodissociation Dynamics of ClF in an Ar Matrix, *Phys. Chem. Chem. Phys.* **2002**, *4*, 5554-5562.

- (12) Kawarai, Y.; Weber, T.; Azuma, Y.; Winstead, C.; McKoy, V.; Belkacem, A.; Slaughter, D. S. Dynamics of the Dissociating Uracil Anion Following Resonant Electron Attachment. *J. Phys. Chem. Lett.* **2014**, *5*, 3854-3858.
- (13) García-Vela, A.; Henriksen, N. E. Coherent Control of Photofragment Distributions Using Laser Phase Modulation in the Weak-Field Limit. *J. Phys. Chem. Lett.* **2015**, *6*, 824-829.
- (14) Geißler, D.; Marquetand, P.; González-Vázquez, J.; González, L.; Rozgonyi, T.; Weinacht, T. Control of Nuclear Dynamics with Strong Ultrashort Laser Pulses. *J. Phys. Chem. A* **2012**, *116*, 11434-11440.
- (15) Clarkson, J. R.; Herbert, J. M.; Zwier, T. S. Infrared Photodissociation of a Water Molecule from a Flexible Molecule-H<sub>2</sub>O Complex: Rates and Conformational Product Yields Following XH Stretch Excitation. *J. Chem. Phys.* **2007**, *126*, 134306-1-15.
- (16) Han, Y. C.; Shepler, B. C.; Bowman, J. M. Quasiclassical Trajectory Calculations of the Dissociation Dynamics of CH<sub>3</sub>CHO at High Energy Yield Many Products. *J. Phys. Chem. Lett.* **2011**, *2*, 1715C1719.
- (17) Shu, C. C.; Rogonyi, T.; González, L.; Henriksen, N. E.; A Theoretical Investigation of the Feasibility of Tannor-Rice Type Control: Application to Selective Bond Breakage in Gas-Phase Dihalomethanes. *J. Chem. Phys.* **2012**, *136*, 174303-1-9.
- (18) Yuan, J.-M.; George, T. F.; Semiclassical Theory of Unimolecular Dissociation Induced by a Laser Field. *J. Chem. Phys.* **1981**, *74*, 1110-1117.
- (19) Bandrauk, A. D.; Sink, M. L. Photodissociation in Intense Laser Fields: Predissociation Analogy Semiclassical Theory of Unimolecular Dissociation Induced by a Laser Field. *J. Chem. Phys.* **1978**, *68*, 3040-3052.
- (20) Aubanel, E. E.; Bandrauk, A. D. Rapid Vibrational Inversion via Time Gating of Laser-

- Induced Avoided Crossings in High-Intensity Photodissociation. *J. Chem. Phys.* **1993**, *97*, 12620-12624.
- (21) Chang, B. Y.; Shin, S.; Santamaria, J.; Sola, I. R. Bond Breaking in Light-Induced Potentials. *J. Chem. Phys.* **2009**, *130*, 124320-1-9.
- (22) Bucksbaum, P. H.; Zavriyev, A.; Muller, H. G. Softening of the  $H_2^+$  Molecular Bond in Intense Laser Fields. *Phys. Rev. Lett.* **1990**, *64*, 1883-1886.
- (23) Frasiniski, L. J.; Posthumus, J. H.; Plumridge, J.; Codling, K.; Taday, P. F.; Langley, A. J. Manipulation of Bond Hardening in  $H_2^+$  by Chirping of Intense Femtosecond Laser Pulses. *Phys. Rev. Lett.* **1999**, *83*, 3625-3628.
- (24) Giusti-Suzor, A.; He, X.; Atabek, O.; Mies, F. H. Above-Threshold Dissociation of  $H_2^+$  in Intense Laser Fields. *Phys. Rev. Lett.* **1990**, *64*, 515-518.
- (25) Orr, P. A.; Williams, I. D.; Greenwood, J. B.; Turcu, I. C. E.; Bryan, W. A.; Pedregosa-Gutierrez, J.; Walter, C. W. Above Threshold Dissociation of Vibrationally Cold  $HD^+$  Molecules. *Phys. Rev. Lett.* **2007**, *98*, 163001-1-4.
- (26) Halász, G. J.; Vibók, Á.; Cederbaum, L. S. Direct Signature of Light-Induced Conical Intersections in Diatomics. *J. Phys. Chem. Lett.* **2015**, *6*, 348-354.
- (27) Moiseyev, N.; Sindelka, M.; Cederbaum, L. S. Laser-Induced Conical Intersection in Molecular Optical Lattices. *J. Phys. B* **2008**, *41*, 221001-1-5.
- (28) Sindelka, M.; Moiseyev, N.; Cederbaum, L. S. Strong Impact of Light-Induced Conical Intersections on the Spectrum of Diatomic Molecules. *J. Phys. B* **2011**, *44*, 045603-1-6.
- (29) Cederbaum, L. S.; Chiang, Y. C.; Demekhin, P. V.; Moiseyev, N. Resonant Auger Decay of Molecules in Intense X-Ray Fields: Light-Induced Strong Nonadiabatic Effects. *Phys. Rev. Lett.* **2011**, *106*, 123001-1-4.

- (30) Halász, G. J.; Sindelka, M.; Moiseyev, N.; Cederbaum, L. S.; Vibók, Á. Light-Induced Conical Intersections: Topological Phase, Wave Packet Dynamics, and Molecular Alignment. *J. Phys. Chem. A* **2012**, *116*, 2636-2643.
- (31) Halász, G. J.; Vibók, Á.; Meyer, H. D.; Cederbaum, L. S. Effect of Light-Induced Conical Intersection on the Photodissociation Dynamics of the  $D_2^+$  Molecule. *J. Phys. Chem. A* **2012**, *117*, 8528-8535.
- (32) Halász, G. J.; Csehi, A.; Vibók, Á.; Cederbaum, L. S. Influence of Light-Induced Conical Intersection on the Photodissociation Dynamics of  $D_2^+$  Starting from Individual Vibrational Levels. *J. Phys. Chem. A* **2011**, *116*, 11908-11915.
- (33) Csehi, A.; Halász, G. J.; Cederbaum, L. S.; Vibók, Á. Towards Controlling the Dissociation Probability by Light-Induced Conical Intersections. *Faraday Discuss.* **2016**, DOI: 10.1039/c6fd00139d.
- (34) Natan, A.; Ware, M. R.; Prabhudesai, V. S.; Lev, U.; Bruner, B. D.; Heber, O.; Bucksbaum, P. H. Observation of Quantum Interferences via Light-Induced Conical Intersections in Diatomic Molecules. *Phys. Rev. Lett.* **2016**, *116*, 143004-1-5.
- (35) Rose, T. S.; Rosker, M. J.; Zewail, A. H. Femtosecond Real-Time Probing of Reactions. IV. The Reactions of Alkali Halides. *J. Chem. Phys.* **1989**, *91*, 7415-7436.
- (36) Bandrauk, A. D.; Child, M. S. Analytic Predissociation Linewidths from Scattering Theory. *Mol. Phys.* **1970**, *19*, 95-111.
- (37) Shu, C.-C.; Henriksen, N. E. Coherent Control of Indirect Photofragmentation in the Weak-Field Limit: Control of Transient Fragment Distributions. *J. Chem. Phys.* **2011**, *134*, 164308-1-8.
- (38) Shu, C.-C.; Yu, J.; Yuan, K.-J.; Hu, W. H.; Yang, J.; Cong, S. L. Stimulated Raman adiabatic passage in molecular electronic states. *Phys. Rev. A* **2009**, *79*, 023418-1-10.

- (39) Henriksen, N. E. A Theoretical Analysis of Time-Dependent Fragment Momenta in Indirect Photofragmentation. *J. Chem. Phys.* **2010**, *132*, 234311-1-4.